Ultramicroscopy 205 (2019) 1–4

Contents lists available at ScienceDirect

Ultramicroscopy

journal homepage: www.elsevier.com/locate/ultramic

Calibrating lateral displacement sensitivity of AFM by stick-slip on stiff, amorphous surfaces

Liangyong Chu[*,a,b], Marcel Bus[a], Alexander V. Korobko[a], Nicolaas A.M. Besseling[a]

[a] Organic Materials and Interfaces, Department of Chemical Engineering, Delft University of Technology, van der Maasweg 9, Delft 2629 HZ, the Netherlands
[b] Surface Technology and Tribology, Department of Mechanics of Solids, Surfaces and Systems (MS3), University of Twente, Drienerlolaan 5, Enschede 7522 NB, the Netherlands

ARTICLE INFO

Keywords:
AFM
Lateral force
Calibration
Contact stiffness

ABSTRACT

We calibrate the lateral mode AFM (LFM) by determining the position-sensitive photodetector (PSPD) signal dependency on the lateral tip displacement, which is analogous to the constant-compliance region in normal-force calibration. By stick-slip on stiff, amorphous surfaces (silica or glass), the lateral tip displacement is determined accurately using the feedback loop control of AFM system. The sufficiently high contact stiffness between the Si AFM tip and stiff, amorphous surfaces substantially reduces the error of PSPD signal dependency on the lateral tip displacement. No damage or modification of the AFM probe is involved and only a clean silicon or glass wafer is needed.

1. Introduction

Precise measurement of nanoscale friction forces is important, for both fundamental understanding and many practical applications [1–7]. The effect of friction forces has been extensively studied in the last decades, especially in relation to lubrication [8,9], micro (nano)-electro-mechanical systems (MEMS&NEMS) [10], nano-tribology [7,11–14] and earthquakes [15,16]. Since the 1960s, various instruments including the surface force apparatus (SFA), the atomic force microscope (AFM), and the quartz microbalance have been applied to study friction at the micro- to the nanoscale [15,17]. Lateral force mode AFM (LFM), measuring the ultra-small lateral forces (nN to μN) between the AFM tip and the sample surface, is the most popular method in this field [15,18,19]. Especially, it has become increasingly popular to understand earthquakes at nanoscale contacts. As it has been shown by Li et al. using LFM, the formation of interfacial chemical bonds is qualitatively responsible for frictional ageing in macroscopic rock friction experiments [16]. A problem with LFM, as opposed to AFM normal force measurements, is that LFM is not readily calibrated. That hampers the measurement of accurate absolute values for the lateral forces [20]. For not too large lateral tip displacements Δx_t, the lateral force F_x exerted by the tip on the sample surface, due to a twist of the cantilever, is proportional to Δx_t [21]:

$$F_x = -K_x \Delta x_t. \tag{1}$$

The twist of the cantilever also leads to a change of the lateral signal of the PSPD. For not too large Δx_t, the signal is linear in the tip displacement:

$$\Delta I_x = \sigma_x \Delta x_t, \tag{2}$$

where σ_x is the sensitivity coefficient. The displaced positions of the sample and the tip are indicated by the dashed contours as shown in Fig. 1. In the sketch, $\Delta x_t < \Delta x_s$, which implies that some slip of the tip over the sample has occurred. The slip distance is $\Delta x_t - \Delta x_s$. In this drawing, as with the experiments described in this Letter, the sample is laterally displaced with respect to the neutral tip position by a piezo scanner on which the sample is mounted. Obviously, a setup, in which a piezo scanner connected to its base laterally displaces the cantilever with respect to a stationary sample, is equivalent.

So, to get the force from a certain tip displacement, one needs to know the spring constant K_x. As for the normal forces, the “thermal-noise method” seems a convenient way to determine the spring constant [22]. This method obtains the spring constant from the thermal fluctuations of the tip displacement of a free-standing probe. For a harmonic potential, $U_x = K_x \Delta x_t^2/2$, consistent with Eq. (1), the mean square of the fluctuating tip displacements at thermal equilibrium is given by

$$\overline{\Delta x_t^2} = k_B T / K_x, \tag{3}$$

where T is the temperature, and k_B is Boltzmann’s constant. The

* Corresponding author at: Organic Materials and Interfaces, Department of Chemical Engineering, Delft University of Technology, van der Maasweg 9, 2629 HZ Delft, the Netherlands.
E-mail addresses: L.Chu@utwente.nl (L. Chu), klaas.besseling@gmail.com (N.A.M. Besseling).

https://doi.org/10.1016/j.ultramic.2019.05.012
Received 3 October 2018; Received in revised form 17 April 2019; Accepted 24 May 2019
Available online 25 May 2019

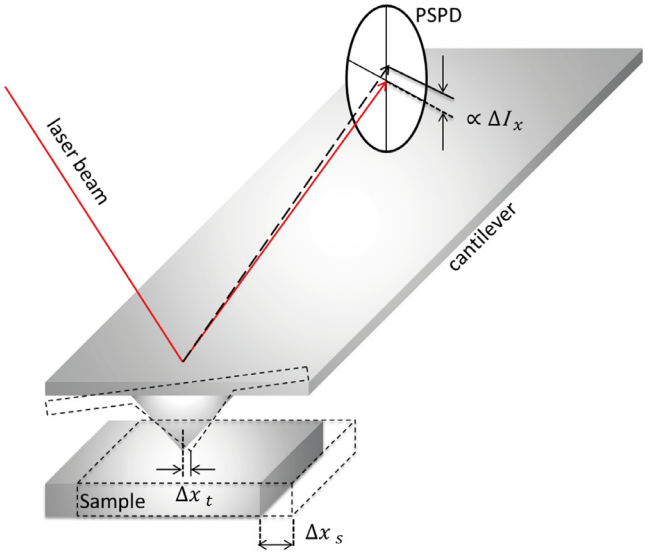

Fig. 1. (Color online) Schematic drawing of the LFM system (not to scale). The actual length, width and tip height of the probe are typically 100–400 μm, 30–60 μm, and 5–15 μm respectively. The distance to the position-sensitive photodetector (PSPD) is much larger than that, whereas the lateral displacement Δx_s of a piezo scanner and the sample mounted on it is only 6 nm at maximum in the experiments described in this article. As the sample travels laterally by a distance Δx_s, the tip displaces laterally by Δx_t with respect to its neutral position, as it is "dragged along" by the sample. Then the cantilever gets twisted, leading to a lateral force by the tip upon the sample. (For interpretation of the references to color in this figure legend, the reader is referred to the web version of this article.)

harmonic oscillator spring constant K_x is determined by both the stiffness of the cantilever and the tip. Thus, this expression also applies when the tip stiffness is comparable to the cantilever stiffness and both springs work in the linear region [23]. So, when we know $\overline{\Delta x_t^2}$ from a measurement of the tip-position fluctuations, we also know the sought for spring constant, K_x. As recognized by Hutter et al., $\overline{\Delta x_t^2}$ is best determined as the integral of the resonance peak in the power spectrum density [24].

However, the problem is that we cannot directly measure Δx_t values. Rather, we measure the signal of the position-sensitive photodetector (PSPD) (see Fig. 1) $\Delta I_x = I_x - I_{x,0}$ where I_x is the PSPD lateral-signal readout, and $I_{x,0}$ its mean value when no external forces, *e.g.* due to interactions with a sample, work on the tip.

With AFM normal-force measurements, the sensitivity coefficient is obtained from the so-called "constant-compliance" or "contact" region of a measured dependency of the PSPD signal vs. piezo-displacement [20,25]. In this region, the tip displacement follows exactly that of the piezo scanner on which the sample is mounted, and the sensitivity coefficient is simply the slope of the signal vs. piezo-displacement curve. For lateral-force experiments, it has thus far not been possible to accurately measure something analogous to the constant-compliance dependency in normal-force experiments [26]. To obtain a similar constant-compliance dependency in lateral force measurement, the tip needs to stick perfectly to the sample, and the PSPD signal ΔI_x, when the sample mounted on the scanner has a displacement of Δx_s, needs to be determined.

Salmeron group determined the lateral sensitivity coefficient σ_x, based on the stick-slip behavior when AFM tip slides on a muscovite mica surface [26]. Δx_s can be well obtained since the lattice parameter of mica surface is known. In principle, σ_x is derived as the slope of the stick-slip signal, since the tip sticks to the surface at "stick" region. They have proved that this method leads to a big error in the results, as the contact stiffness is lower compared to the cantilever stiffness [26]. Because of a very low shear modulus and the layered structure of mica, sufficient contact stiffness cannot be achieved by simply increasing the normal load force [9]. Generally, the contact stiffness can be increased by materials having larger shear modulus, *e.g.* Si. However, the stick-slip behavior on Si with a native silica layer is chaotic, Δx_t cannot be determined in the same way as that on crystallized mica surface. Salmeron group reported the LFM calibration based on the measured correlation between the lateral signal and normal load forces [27]. For that, the AFM probe slides across a surface with a defined slope. However, this "wedge" method requires a surface with well-defined atomic scale slope. A number of publications have addressed the issue of LFM calibration. Bogdanovic et al. measured the torsional spring constant of a tipless cantilever by pushing it against a sharp upwards pointing tip. If the tip contacts the corner of the cantilever, the torsional spring constant can be obtained [28]. The accuracy is high but the method can only be used for tipless cantilevers and additional information about tip height is desired. Cannara et al. determined the sensitivity, by gluing a colloidal sphere to the probe and pushing the sphere against a wall to get the ΔI_x vs. Δx curve [29]. Feiler et al. twisted the cantilever by attaching a mass at one side using a glass fibre [30]. These direct ways are accurate but they require modification or damaging of the probe [31]. Furthermore, in order to obtain the proportionality constant between the force and the actual tip displacement (as in Eq. (1)), additional tip-height data is needed [27,32]. The lateral spring constant can also be calculated from the dimensions of the cantilever [33,34]. However, the accuracy is low due to inaccuracies of these dimensions. Sader made significant and widely used contributions by analyzing the cantilever resonance frequency shift in vacuum and air, only cantilever's plan view dimensions are needed [35,36].

Herein, we present a simple method to calibrate lateral-force AFM. A Si wafer with high shear modulus is used to ensure the high contact stiffness and negligibly small contact deformation of a substrate. The accurate control of tip displacement is achieved with the closed-loop X-Y control of the AFM instrument [37,38], and it works on typical commercial AFM instruments. The method yields directly the proportionality constant between the lateral tip displacement and the lateral force as Eq. (1) predicts, without the need for further geometrical calculations of the tip, which would introduce additional errors. No modifications of the probes are required.

2. Results and discussions

Fig. 2(a) shows two typical lateral-signal traces for the sliding of a Si AFM tip with a very low scan speed over a small distance across a silica surface. The normal load forces are 0 and -1 nN (a negative normal load corresponds to a force pulling the tip from the surface; tip-surface contact is maintained by adhesive interactions, the adhesive force between the tip and sample is about 2 nN, determined from the normal force distance curve). The small (or even negative) normal loads ensure that the tip is not damaged due to wear, as the contact stress is lower than the yield stress of silica. This is further confirmed by the fact that the signal shift after 512 scans is negligible, as shown in Fig.S2. After averaging over 512 scans, stepwise motion of the piezo scanner is reviled as shown in Fig. 2(b). With the current settings, the change of $\langle \Delta x_s \rangle$ from 0 to 6.1 nm in 5 s is achieved in 11 steps, as shown in the blue and red lines in Fig. 2(b), numbered as 1–11. So, each $\langle \Delta x_s \rangle$ step has a magnitude of 0.555 nm, and the time interval between steps is 0.455 s (5 s for 11 steps). The magnitudes of the piezo-scanner steps and the time intervals are controlled by the closed-loop settings of the AFM instrument. The black step-like dashed line in Fig. 2(b) corresponds to the ideal limit of no slip at the interface between AFM tip and silica surface, so that the tip would move with the sample connected to the piezo scanner ($\Delta x_t = \Delta x_s$). The $\langle \Delta x_t \rangle$ axis on the right is constructed by realizing that over the full 5 s the piezo displacement increases from 0 to 6.1 nm (on average), and by taking into account that for the no-slip case $\Delta x_t = \Delta x_s$. The difference $\langle \Delta x_t \rangle - \langle \Delta x_s \rangle$ corresponds to the distance

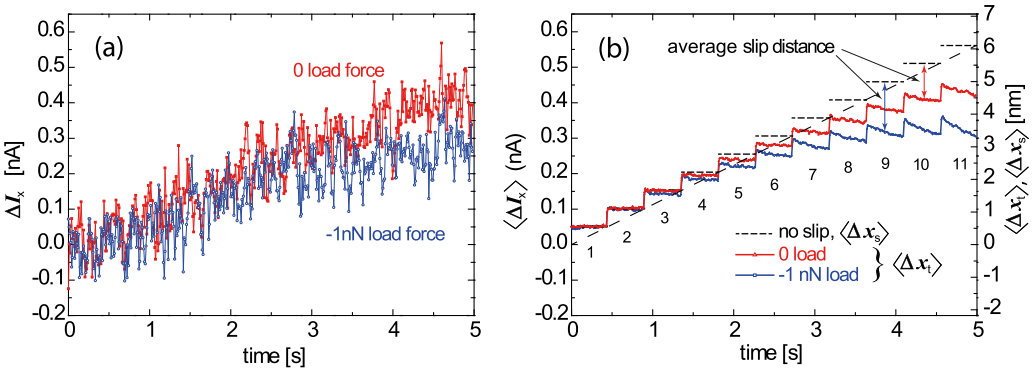

Fig. 2. (Color online) (a) The lateral signal ΔI_x as a function of time for single scans with a range of 6.1 nm (see Supporting Information 1). The scan frequency was set at 0.1 Hz (10 s for the trace and retrace), so the duration of a single scan, during which Δx_s varies from 0 to 6.1 nm, is 5 s, and the average scan speed is 1.22 nm/s. 512 points are gathered in a single scan. The feedback loop controlling the tip-sample distance was operated very slowly, in order to avoid any influence on the lateral signals (see Supporting Information 2, Fig. S2.) [39]. (b) Average data of 512 scans at the same normal loads as in (a). $\langle \Delta I_x \rangle(t) = N^{-1} \sum_{i=1}^{N} \Delta I_x(t)_i$, where t denotes time ($0 \le t \le 5$ sec.), N is the total number of scans, (=512), and i is the scan number. The right y axis shows the tip displacement Δx_t according to Eq. (2) and σ_x given below. (For interpretation of the references to color in this figure legend, the reader is referred to the web version of this article.)

that the tip has on average slipped over the sample surface. Moreover, the average scan speed is derived from the slope of the long dashed line.

Accurate nanometer-scale displacement of the scanner is achieved by the closed-loop X-Y control of the AFM instrument, based on an independent capacitive position sensor [37,38], as used in most commercial AFM systems. The feedback from the position sensor ensures the controller to reach and maintain a position set-point during the scanning. At very low scan speeds with closed-loop X-Y control, the piezo scanner in fact moves on average in a stepwise fashion, in which after fixed time intervals the target position of the piezo scanner changes to a new value, while the control loop tries to realize the target position. The noise in Fig. 2(a) is due to noise of the sample position owing to this control system. All the instrumental noises including noises from the positioning control system, the environmental vibrations, and voltage fluctuations do not influence the stick-slip experiment, thus their average values over scans are considered to be fixed. The scan rate here is much lower than the scan rate which is common with small-scale scanning and imaging. For typical nanoscale mapping, much higher scan speeds (*e.g.* 60 Hz for a 10 nm scan) are needed to get a high linear position control [40].

We see in Fig. 2(a) that, apart from the fluctuations, the lateral signal initially increases linearly, and levels off later on. For a -1 nN normal load this leveling off becomes noticeable beyond about 2 s. For a zero normal load, leveling off occurs later and is less pronounced. It is appealing to infer that initially the lateral force F_x does not exceed the static friction force, so that the signal corresponds to the tip displacement Δx_t following the sample displacement, which equals Δx_s. This would mean that this part of the trace is analogous to the constant-compliance region in a normal-force analysis. Hence, in principle, the sensitivity $\sigma_x = \Delta I_x/\Delta x_t$ can be obtained from the initial slope of these traces, taking into account that the Δx_s increases from 0 to 6.1 nm over 5 s. However, due to the fluctuations, which are of the same order of magnitude as the trend-like change of ΔI_x, the relative error would be substantial. Not using the control loop reduces the fluctuation, but leads to an unacceptable uncertainty in the lateral position.

For the cases shown in Fig. 2, the virtually vertical steps of the averaged signal $\langle \Delta I_x \rangle$ all have the same magnitude, indicating that during the steps no slip occurs [41]. Hence, the change of the tip's average displacement upon a step, $\Delta\langle \Delta x_t \rangle$, equals the change of the average piezo-scanner displacement $\Delta\langle \Delta x_s \rangle$ upon a step. In this way, the accurate control of the tip's average displacement is achieved on an amorphous surface. We want to point out that this approach is different from determining the lateral displacement from the stick-slip on surfaces with well-defined periodic structure [26].

During the time intervals between the steps we observe either a virtually constant signal, or some decay of the signal. These decays are negligible for the first intervals, but become more pronounced as the signal and hence the lateral force increases. Furthermore, these decays are more pronounced for the -1 nN normal load than for the zero normal load. The decay is obviously due to slip of the tip over the sample surface, upon which $\langle \Delta x_t \rangle$ and hence $\langle \Delta I_x \rangle$ decreases. In fact, these decay curves are averages over many stick-slip type events occurring in the separate scans of which Fig. 2(b) shows the average ΔI_x. These traces contain force relaxation information on nano-frictional behavior and will be published in details elsewhere. As reported by Salmeron's group, the calibration of Lateral Force fails when the contact and cantilever stiffnesses are comparable. The deformation of the substrate at contact leads to a big error of the lateral sensitivity [26]. This problem cannot be solved by simply increasing the normal load force, due to the layered structure of mica. Egberts reported a similar lateral calibration as function of normal load on potassium bromide (KBr) surface, probably because the insufficient stiffness of the substrate [42]. Herein, we demonstrated that this problem can be avoided with using the amorphous stiff silica surface. Fig. 3 shows $\Delta\langle \Delta I_x \rangle$ of the first step (the change of $\langle \Delta I_x \rangle$ corresponding to a single step of length) versus the normal load force. Two probes with different stiffness are used. The soft probe is a commercial LFM probe with the normal spring constant of 0.2 N/m (determined by the thermal noise method). The

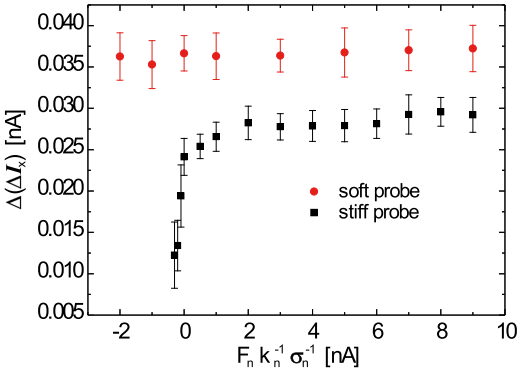

Fig. 3. (Color online) $\Delta\langle \Delta I_x \rangle$ (the change of $\langle \Delta I_x \rangle$ corresponding to a single step of length) versus normal load force data on silica surface using probes with different stiffness. Load forces ranging from minimum, corresponding to the jump-out force and maximum, corresponding to the maximum linear response range of the PSPD (see Supporting Information 3) are used. $F_n K_n^{-1} \sigma_n^{-1}$ is the normalized normal load force, corresponding to the output of the PSPD [20]. The error is calculated from the data of each step. For the glass surface, $\Delta\langle \Delta I_x \rangle$ versus normal load force is shown in Supporting Information 6. (For interpretation of the references to color in this figure legend, the reader is referred to the web version of this article.)

stiff probe is a standard tapping mode probe with the normal spring constant 4.7 N/m (determined by the thermal noise method). As shown in Fig. 3, for the soft LFM probe, the step size $\Delta\langle\Delta I_x\rangle$ keeps constant with the increase of the load force. This indicates the contact stiffness is much larger than the spring constant of the probe and the contact deformation is negligible with respect to Δx_s in the whole load force range. For the stiff probe, the step size $\Delta\langle\Delta I_x\rangle$ increases sharply and levels off with the increasing load force. In this case, the contact stiffness at smaller normal load force is comparable to the stiffness of cantilever and the contact deformation cannot be neglected. Irrelevantly the stiffness, the step-size becomes constant for large normal load forces, indicating that using silica surface sufficient contact stiffness between tip and sample is ensured. Thus, for the stiff cantilever calibration, the change of $\langle\Delta I_x\rangle$ corresponding to a single step of length versus normal load force data needs to be checked as shown in Fig. 3. Following the increase of the normal load, the step size $\Delta\langle\Delta I_x\rangle$ firstly increases sharply and we get the accurate lateral displacement sensitivity when $\Delta\langle\Delta I_x\rangle$ levels off.

As $\Delta\langle\Delta x_t\rangle = \Delta\langle\Delta x_s\rangle$ for the vertical steps of the averaged signal we can readily calculate the sensitivity coefficient. First we determine the change of $\langle\Delta I_x\rangle$ corresponding to a single step of length $\Delta\langle\Delta x_s\rangle = 0.555$ nm. By taking the average over all steps in the measurement, we find that the signal change for a single step is $\Delta\langle\Delta I_x\rangle = 0.051 \pm 0.002$ nA. The error is calculated as the standard deviation over these 11 steps. So we calculate the lateral sensitivity coefficient realizing that $\sigma_x = \Delta\langle\Delta I_x\rangle/\Delta\langle\Delta x_s\rangle = (0.051 \pm 0.002)$ nA/0.555 nm =0.092 ± 0.004 A/m.

The “no-slip trace” in Fig. 2(b) (black short-dashed line) was constructed using this same $\Delta\langle\Delta I_x\rangle$ value of 0.051 nA per step. The difference between this constructed no-slip trace and an experimental trace yields the distance that the tip has slipped over the surface (averaged over all scan repeats): $\langle x_t\rangle - \langle x_s\rangle = \sigma_x(\langle\Delta I_x\rangle_{\text{exp}} - \langle\Delta I_x\rangle_{\text{noslip}})$.

Knowing the lateral sensitivity, the lateral spring constant of the probe, as defined by Eq. (1), can be readily determined, *e.g.* using the thermal-noise method as mentioned above. For the present case, for the free standing probe (not interacting with any sample), at room temperature ($T = 299.0$ K), $\overline{\Delta x_t^2}$ is determined as $(3.2 \pm 0.1)\cdot 10^{-21}$ m^2 (see Supporting Information 4) [22]. With Eq. (3) we obtain $K_x = k_B T/\overline{\Delta x_t^2} = 1.29 \pm 0.04$ N/m, which does not depend on the alignment. The error is calculated as $\varepsilon_{\sigma_x}\partial K_x/\partial\sigma_x$, where ε_{σ_x} is the standard deviation of the sensitivity coefficient σ_x. Thus, $F_x = K_x/\sigma_x\cdot\Delta I_x = k_B T/\overline{\Delta I_x^2}\cdot\sigma_x\Delta I_x = (14.2 \pm 0.6)\Delta I_x$, the error of the coefficient K_x/σ_x is determined as $k_B T/\overline{\Delta I_x^2}\varepsilon_{\sigma_x}$. Apparently, as shown in Supporting Information 7, K_x only depends on the probe and temperature, being insensitive to the experimental AFM system.

3. Conclusion

In conclusion, we have developed the simple method to calibrate the LFM system by determining the PSPD signal dependency on the lateral tip displacement, which is analogous to the constant-compliance region in normal-force calibration. To suppress the error owing to low contact stiffness, an amorphous surface (silica or glass) ensuring sufficiently high contact stiffness between the Si AFM tip and sample is used. The lateral tip displacement is determined by stick-slip on stiff, amorphous surfaces using the feedback loop control of AFM system. In our LFM calibration method, only a clean silicon or glass wafer is required, and it works on conventional commercial AFM.

Acknowledgment

We acknowledge the PhD Scholarship of L.C. from the China Scholarship Council of the Ministry of Education of China (No. 201306450011).

Supplementary material

Supplementary material associated with this article can be found, in the online version, at 10.1016/j.ultramic.2019.05.012 .

References

[1] F. Chen, U. Mohideen, G.L. Klimchitskaya, V.M. Mostepanenko, Phys. Rev. Lett. 88 (2002) 101801.
[2] E. Riedo, E. Gnecco, R. Bennewitz, E. Meyer, H. Brune, Phys. Rev. Lett. 91 (2003) 084502.
[3] T. Filleter, J.L. McChesney, A. Bostwick, E. Rotenberg, K.V. Emtsev, T. Seyller, K. Horn, R. Bennewitz, Phys. Rev. Lett. 102 (2009) 086102.
[4] A. Buldum, J.P. Lu, Phys. Rev. Lett. 83 (1999) 5050.
[5] K.B. Jinesh, J.W.M. Frenken, Phys. Rev. Lett. 96 (2006) 166103.
[6] T. Baumberger, C. Caroli, Adv. Phys. 55 (2006) 279.
[7] S.Y. Krylov, J.W.M. Frenken, Phys. Status Solidi B 251 (2014) 711.
[8] M. Dienwiebel, G.S. Verhoeven, N. Pradeep, J.W.M. Frenken, J.A. Heimberg, H.W. Zandbergen, Phys. Rev. Lett. 92 (2004) 126101.
[9] S. Minko, M. Müller, D. Usov, A. Scholl, C. Froeck, M. Stamm, Phys. Rev. Lett. 88 (2002) 035502.
[10] B. Wen, J.E. Sader, J.J. Boland, Phys. Rev. Lett. 101 (2008) 175502.
[11] E. Meyer, R. Overney, D. Brodbeck, L. Howald, R. Lüthi, J. Frommer, H.J. Güntherodt, Phys. Rev. Lett. 69 (1992) 1777.
[12] S. Ge, Y. Pu, W. Zhang, M. Rafailovich, J. Sokolov, C. Buenviaje, R. Buckmaster, R.M. Overney, Phys. Rev. Lett. 85 (2000) 2340.
[13] M. Enachescu, R.J.A. van den Oetelaar, R.W. Carpick, D.F. Ogletree, C.F.J. Flipse, M. Salmeron, Phys. Rev. Lett. 81 (1998) 1877.
[14] Y. Liu, I. Szlufarska, Phys. Rev. Lett. 109 (2012) 186102.
[15] J.N. Israelachvili, Intermolecular and Surface Forces, Academic press, 2011.
[16] Q. Li, T.E. Tullis, D. Goldsby, R.W. Carpick, Nature 480 (2011) 233.
[17] B. Bhushan, J.N. Israelachvili, U. Landman, Nature 374 (1995) 13.
[18] G. Binnig, C.F. Quate, C. Gerber, Phys. Rev. Lett. 56 (1986) 930.
[19] J.P. Salvetat, G.A.D. Briggs, J.M. Bonard, R.R. Bacsa, A.J. Kulik, T. Stöckli, N.A. Burnham, L. Forró, Phys. Rev. Lett. 82 (1999) 944.
[20] H.J. Butt, B. Cappella, M. Kappl, Surf. Sci. Rep. 59 (2005) 1.
[21] Note that, unlike some others, we define K_x and σ_x as proportionality constants between *tip displacement* and the force, and between *tip displacement* and PSPD signal. K_x defined in this way is not simply the spring constant of the cantilever, but is determined by the tip stiffness and height as well. These are the proportionality constants that are actually needed in measurements of *e.g.* friction forces, and that will be determined by our present method.
[22] H.J. Butt, M. Jaschke, Nanotechnology 6 (1995) 1.
[23] M. Lantz, S. Oshea, A. Hoole, M. Welland, Appl. Phys. Lett. 70 (1997) 970.
[24] J.L. Hutter, J. Bechhoefer, Rev. Sci. Instrum. 64 (1993) 1868.
[25] W.A. Ducker, T.J. Senden, R.M. Pashley, Nature 353 (1991) 239.
[26] R.W. Carpick, D. Ogletree, M. Salmeron, Appl. Phys. Lett. 70 (1997) 1548.
[27] D. Ogletree, R.W. Carpick, M. Salmeron, Rev. Sci. Instrum. 67 (1996) 3298.
[28] G. Bogdanovic, A. Meurk, M. Rutland, Colloids Surf B 19 (2000) 397.
[29] R.J. Cannara, M. Eglin, R.W. Carpick, Rev. Sci. Instrum. 77 (2006) 053701.
[30] A. Feiler, P. Attard, I. Larson, Rev. Sci. Instrum. 71 (2000) 2746.
[31] Q. Li, K.S. Kim, A. Rydberg, Rev. Sci. Instrum. 77 (2006) 065105.
[32] H. Wang, M.L. Gee, Ultramicroscopy 136 (2014) 193.
[33] E. Liu, B. Blanpain, J.P. Celis, Wear 192 (1996) 141.
[34] C.P. Green, H. Lioe, J.P. Cleveland, R. Proksch, P. Mulvaney, J.E. Sader, Rev. Sci. Instrum. 75 (2004) 1988.
[35] J.E. Sader, J.W.M. Chon, P. Mulvaney, Rev. Sci. Instrum. 70 (1999) 3967.
[36] J.E. Sader, J. App. Phys. 84 (1998) 64.
[37] H. Philipp, Capacitive position sensor, 2001, US Patent 6,288,707.
[38] B. Borovic, A. Liu, D. Popa, H. Cai, F. Lewis, J. Micromech, Microeng 15 (2005) 1917.
[39] A. Socoliuc, R. Bennewitz, E. Gnecco, E. Meyer, Phys. Rev. Lett. 92 (2004) 134301.
[40] B. Bhushan, Springer Handbook of Nanotechnology, Springer Science & Business Media, 2010.
[41] That for those cases no slip occurs during the steps, so that the tip follows the sample, is essential for the further argument. There are in fact several observations that indicate that this is indeed true: If slip would occur, increase of the lateral force should increase the slip distance, and the observed step length would decrease. This is not observed. Furthermore, increase of the normal load should reduce slip, and hence increase the observed step lengths. Also this is not observed for this system. We have made tests with “more slippery” surfaces (mica, gold, graphene), and for those, we do observe such signatures of slip occurring during the steps.
[42] P. Egberts, Nanotechnology 22 (2011) 425703.